TO REFEREE #2

Thank you very much for all your suggestions and comments. Next, we respond all your suggestions in order.

1. With respect to the differences found between the use of Normal distributions and GEV distributions, could authors affirm that such differences are statistically significant?:
   We recognize the limitations of this study in the selected time period. We were limited to work with 16 years and approximately 96 observations per RV. However, we have found that observed NDVI distributions are mainly asymmetric in spring and autumn, inconsistent with symmetric Normal fitting.
   In addition, we have included that the level of significance of the Chi-Square fit was fixed to 5% for all the candidates (this information did not appear in the first version and it will be included now).
   Anyway, the objective of this study is to generate some reasonable doubts about the convenience of using Normal distributions in all cases, and to notice that others alternatives to Normal distributions could exist. GEV distribution is an example of better fit than Normal one with the limitations explained above.
2. Did the authors apply this methodology on geographic areas of different characteristics with respect to the characteristics of the area analyzed in the present study?
   In this study we have only focused on pasture and methodology applicable to calculate damaged pasture thresholds. However, we also think this methodology could be extrapolated to other types of vegetation in further researches.
3. Minor comments:
   a) We have homogenized the term “Normal distribution” to uppercase.
   b) Page 1, line 22: We have inserted Moderate Resolution Imaging Spectroradiometer before MODIS in the Abstract.
   c) Page 4, line 151: We have deleted the definition of MODIS.
   d) Page 6, line 235: We have deleted the definition of MODIS.
   e) Page 7, line 263: We have added mm after 360.
   f) Page 8, line 275: We have inserted “,”.
   g) Page 8, Table 1: We have deleted the dot.
   h) Page 10, line 346: We have modified the equation (7).
   i) Page 11, line 358: We have modified the graphs and included the scale and name of axis.
   j) Page 14, line 435: We have also modified this graph and the figure caption.
   k) We have reviewed the format references.

Statistical Analysis for Satellite Index-Based Insurance to define Damaged Pasture Thresholds

Juan José Martín-Sotoca[1]*, Antonio Saa-Requejo[2,3], Rubén Moratiel[2,3], Nicolas Dalezios[4], Ioannis Faraslis[5], and Ana María Tarquis[2,6]

jmartinsotoca@gmail.com, antonio.saa@upm.es, ruben.moratiel@upm.es, dalezios.n.r@gmail.com, faraslisgiannis@yahoo.gr, anamaria.tarquis@upm.es

[1] Data Science Laboratory. European University, Madrid, Spain.
[2] CEIGRAM, Research Centre for the Management of Agricultural and Environmental Risks, Madrid, Spain.
[3] Dpto. Producción Agraria. Universidad Politécnica de Madrid, Spain.
[4] Department of Civil Engineering. University of Thessaly, Volos, Greece.
[5] Department of Planning and Regional Development. University of Thessaly, Volos, Greece.
[6] Grupo de Sistemas Complejos. Universidad Politécnica de Madrid, Spain.

* Correspondence to: jmartinsotoca@gmail.com

Abstract: Vegetation indices based on satellite images, such as Normalized Difference Vegetation Index (NDVI), have been used in countries like USA, Canada and Spain for damaged pasture and forage insurance for the last years. This type of agricultural insurance is called "satellite index-based insurance" (SIBI). In SIBI, the occurrence of damage is defined through NDVI thresholds mainly based on statistics derived from Normal distributions. In this work a pasture area at the north of Community of Madrid (Spain) has been delimited by means of Moderate Resolution Imaging Spectroradiometer (MODIS) images. A statistical analysis of NDVI histograms was applied to seek for the best statistical distribution using maximum likelihood method. The results show that the Normal distribution is not the optimal representation and the General Extreme Value (GEV) distribution presents a better fit through the year. A comparison between Normal and GEV are showed respect to the probability under a NDVI threshold value along the year. This suggests that a priori distribution should not be selected and a percentile methodology should be used to define a NDVI damage threshold rather than the average and standard deviation, typically of Normal distributions.

Keywords: NDVI, pasture insurance, GEV distribution, MODIS.

Highlights

- **General Extreme Value (GEV) distribution provides the best fit to the NDVI historical observations.**
- **Difference between Normal and GEV distributions are higher during spring and autumn, transition periods in the precipitation regimen.**
- **NDVI damage threshold shows evident differences using Normal and GEV distributions covering both the same probability (24.20%).**

- **NDVI damage threshold values based on percentiles calculation is proposed as an improvement in the index based insurance in damaged pasture.**

1. Introduction

Agricultural insurance addresses the reduction of the risk associated with crop production and animal husbandry. The concept of index-based insurance (IBI) attempts to achieve settlements based on the value taken by an objective index rather than on a case-by-case assessment of crop or livestock losses (Gommes and Kayitakier, 2013). Indeed, the goal of IBI policy remains to develop an affordable tool to all producers, including smallholders. Specifically, IBI can constitute a safety net against weather-related risks for all members of the farming community, thereby increasing food security and reducing the vulnerability of rural populations to weather extremes. Moreover, IBI can be associated with credits for insured smallholders, due to the fact that the risk of non-repayment for lenders is reduced, which encourages the use of agricultural inputs and equipment, leading to increased and more stable crop production. Over the past decade, the importance of weather index-based insurances (WIBI) for agriculture has been increasing, mainly in developing countries (Gommes and Kayitakier, 2013). This interest can be explained by the potential that IBI constitutes a risk management instrument for small farmers. Indeed, it can be considered within the context of renewed attention to agricultural development as one of the milestones of poverty reduction and increased food security, as well as the accompanying efforts from various stakeholders to develop agricultural risk management instruments, including agricultural insurance products.

Farmers need to protect their land and crops specifically from drought in arid and semi-arid countries, since their production may directly depend mainly on the impacts of this particular natural hazard. Insurance for drought-damaged lands and crops is currently the main instrument and tool that farmers can resort in order to deal with agricultural production losses due to drought. Many of these insurances are using satellite vegetation indices (Rao, 2010), thus they are also called “satellite index-based insurances” (SIBI). SIBI have some advantages over WIBI, such as cost-effective information and acceptable spatial and temporal resolution. They do not, however, resolve the issue of basis risk, i.e. potential unfairness to insurance takers (Leblois, 2012). Moreover, the very nature of an index-based product creates the chance that an insured party may not be paid when they suffer loss. For this reason, in some countries (Spain) they have named this SIBI as “damaged in pasture” to cover not only drought even this one is the main cause.

It is highly recognized that shortage of water has many implications to agriculture, society, economy and ecosystems. Specifically, its impact on water supply, crop production and rearing of livestock is substantial in agriculture. Knowing the likelihood of drought is essential for impact prevention (Dalezios, 2013). Drought severity assessment can be approached in different ways: through conventional indices based on meteorological data, such as temperature, rainfall, moisture, etc. (Niemeyer, 2008), as well as through remote sensing indices based on images usually taken by artificial satellites (Lovejoy et al., 2008) or drones. In the second group they are found Satellite Vegetation Indices (SVI), which can quantify "green vegetation", and soil moisture through Soil Water Index (Gouveia et al., 2009) combining different spectral reflectances. Thus, they are one of the main ways to quantitatively assess drought severity.

At the present time, several satellites (NOAA, TERRA, DEIMOS, etc.) can provide this spectral information with different spatial resolution. Some series with a high temporal frequency are freely available, those from NOAA satellites and Terra. The most widely known SVI is the Normalized Difference Vegetation Index (NDVI). It follows the principle that healthy vegetation mainly reflects the near-infrared frequency band. There are several other important SVI, such as Soil Adjusted Vegetation Index (SAVI) and Enhanced Vegetation Index (EVI) that incorporate soil effects and atmospheric impacts, respectively. An important point of this class of insurance is "when damage occurs". To measure this, a SVI threshold value is defined mainly based on statistics that apply to Normal distributed variables: average and standard deviation. When current SVI values are bellow this threshold value for a period of time, insurance recognizes that a damage is occurring, most of the times drought, and then it begins to pay compensations to farmers.

WIBI aims to protect farmers against weather-based disasters such as droughts, frosts and floods. A WIBI policy links possible insurance payouts with the weather requirements of the crop being insured: the insurer pays an indemnity whenever the realized value of the weather index meets a specified threshold. Whereas payouts in traditional insurance programs are related to actual crop damages, a farmer insured under a WIBI contract may receive a payout. A current difficulty to the wide implementation of WIBI is the weakness of indices. Indeed, there is certainly a need for more efficient indices based on the additional experience gained from the implementation of WIBI products in the developing world. Current trends in index technology are exciting and they actuate high expectations, especially the development of yield indices and the use of remote sensing inputs. Risk protection and insurance illiteracy constitute another difficulty, which has to be addressed by training and awareness-raising at all levels, from farmers to farmers' associations, micro-insurance partners, as well as senior decision-makers in insurance, banking, and

150 politics (Bailey, 2013). It is essential that all stakeholders (especially the insured) perfectly
151 understand the principles of IBI, as otherwise the insurer, even the whole concept of
152 insurance, is at risk of reputation loss for years or decades.
153
154 There is currently a lack of technical capacity in the insurance sectors of most
155 developing countries, which is a constraint to the scaling up and further development of
156 WIBI (Gommes and Kayitakire, 2012). Specifically, although it is possible to design an index
157 product and assist in roll-out, marketing, and sales, such assistance is not possible on a
158 wide scale, simply because there is lack of qualified expertise. Indeed, it usually requires
159 mathematical modeling, data manipulation, and expertise in crop simulation to design an
160 index. Nevertheless, it is possible to structure insurance with multiple indices, but this
161 increases the complexity of the product and makes it difficult for farmers to comprehend
162 it. 'Basis risk' is also a particular problem for index products, which is frequently caused by
163 the fact that measurements of a particular variable, such as rain, may differ at the
164 insurer's measurement site and in the farmer's field. This also creates problems for
165 insurance providers. Indeed, part of the reason the scaling up of index products has failed
166 is that both insurers and farmers suffer from this basis risk.
167
168 Currently, to mitigate impacts of climate-related reduced productivity of French
169 grasslands, several studies have been developed to design new insurance scheme bases
170 indemnity payouts to farmers on a forage production index (FPI) (Rumiguié et al., 2015;
171 2017). Two examples of SIBIs are presented in two different countries: USA and Spain. In
172 particular, in USA there are several insurance programs for pasture, rangeland and forage,
173 which use various indexing systems (rainfall and vegetation indices), and are promoted by
174 Unites States Department of Agriculture (USDA) (Maples et al., 2016; USDA, 2018). NDVI is
175 the index chosen in the vegetation index program and it is obtained from AVHRR
176 (Advanced Very High Resolution Radiometer) sensor onboard NOAA satellites. Average,
177 maximum and minimum NDVI values are obtained from a historical series with the aim of
178 calculating a trigger value. Insurer decides the quantity of compensation comparing this
179 trigger with current value. On the other hand, in Spain there exists the "Insurance for
180 Damaged Pasture" from "Spanish System of Agricultural Insurance" (BOE, 2013). This
181 insurance defines damage event through NDVI values obtained from MODIS sensor
182 onboard TERRA satellite of NASA. In this insurance, NDVI threshold values ($NDVI_{th}$) are
183 calculated subtracting several times ($k = 0.7\ or\ k = 1.5$) standard deviation to average
184 within a homogeneous area:
185
186 $$NDVI_{th} = \mu - k \cdot \sigma \quad (1)$$
187

where μ, σ are average and standard deviation of NDVI respectively. Average and standard deviation come of supposing Normal distributions in the historical data (Goward et al., 1985; Hobbs, 1995; Fuller, 1998; Al-Bakri and Taylor, 2003; Turvey et al., 2012; De Leeuw et al. 2014).

The aim of this paper is to find a more realistic statistical NDVI distribution without the "a priori" assumption that variables follow a Normal distribution, typically for current SIBI methodology. In order to achieve this, the Maximum Likelihood Method (MLM) is fitted to a historical series of NDVI values in a pasture land area in Spain (Community of Madrid). Different types of asymmetrical distributions are examined with the aim to find a better fit than Normal. To eliminate some noise in the historical series, an original method is applied consisting of using Hue-Saturation-Lightness (HSL) color model. Finally, Chi-square test (χ^2 test) has been used to check the goodness of fit for all considered distributions.

2. Materials and Methods

2.1 Vegetation Index

The differences of the reflectance of green vegetation in parts of the electromagnetic radiation spectrum, namely, visible and near infrared, provide an innovative method for monitoring surface vegetation from space. Specifically, the spectral behavior of vegetation cover in the visible (0.4-0.7mm) and near infrared (0.74-1.1mm, 1.3-2.5mm) offers the possibility to monitor from space the changes in the different stages of cultivated and uncultivated plants taking also into account the corresponding behavior of the surrounding microenvironment (Ortega-Farias et al., 2016). Indeed, from the visible part of the electromagnetic radiation spectrum it is possible to draw conclusions about the rate photosynthesis, whereas from near infrared inferences are extracted about the chlorophyll density and the amount of canopy in the plant mass, as well as the water content in the leaves, which is also linked directly to the rate of transpiration with impacts to physiological process of photosynthesis. Usually, data from NOAA/AVHRR series of polar orbit meteorological satellites are used with low spatial resolution (1.1 km^2) and recurrence interval at least twice daily from the same location. Several algorithms combining channels of red (RED), near infrared (NIR) and green (GREEN) have been proposed, which provide indices sensitive to green vegetation.

NDVI uses two frequency bands: red band (660 nm) and near-infrared band (860 nm). Absorption of red band is related to photosynthetic activity and reflectance of near-infrared band is related to presence of vegetation canopies (Flynn, 2006). In drought periods, NDVI values can reduce significantly, therefore many researchers have used this index to measure drought events in recent years (Dalezios et al., 2014). To calculate NDVI we will use this mathematical formula:

$$NDVI = \frac{IR-R}{IR+R} \quad (2)$$

where IR and R are reflectance values in Near-Infrared band and Red band, respectively. NDVI values below zero indicate no photosynthetic activity and are characteristic of areas with large accumulation of water, such as rivers, lakes, or reservoirs. The higher is the NDVI value, the greater is the photosynthetic activity and vegetation canopies.

In this paper, the NDVI is used, which is widely known index with a multitude of applications over time. The NDVI is suited for monitoring of total vegetation, since it partly compensates the changes in light conditions, land slope and field of view (Kundu et al., 2016). In addition, clouds, water and snow show higher reflectance in the visible than in the near infrared, thus, they have negative NDVI values. Indeed, bare and rocky terrain show vegetation index values close to zero. Moreover, the NDVI constitutes a measure of the degree of absorption by chlorophyll in the red band of the electromagnetic spectrum. In summary, the NDVI is a reliable index of the chlorophyll density on the leaves, as well as the percentage of the leaf area density over land, thus, NDVI constitutes a credible measure for the assessment of dry matter (biomass) in various species vegetation cover (Dalezios, 2013). It is clear from the above that the NDVI is an index closely related to growth and development of plants, which can effectively monitor surface vegetation from space.

The continuous increase of the NDVI value during the growing season reflects the vegetative and reproductive growth due to intense photosynthetic activity, as well as the satisfactory correlation with the final biomass production at the end of a growing period. On the other hand, gradual decrease of the NDVI values signifies stress due to lack of water or extremely high temperatures for the plants, leading to a reduction of the photosynthetic rate and ultimately a qualitative and quantitative degradation of plants. NDVI values above zero indicate the existence of green vegetation (chlorophyll), or bare soil (values around zero), whereas values below zero indicate the existence of water, snow, ice and clouds.

2.2 Database

Scientific research satellite Terra (EOS AM-1) has been chosen to provide necessary information to calculate NDVI in the study area. This satellite was launched into orbit by NASA on December 18, 1999. MODIS sensor aboard this satellite collects information of different reflectance bands. MODIS information is organized by "products". The product used in this study was MOD09A1 (LP DAAC, 2014). MOD09A1 incorporates seven frequency bands: Band 1 (620-670 nm), band 2 (841-876 nm), band 3 (459-479 nm), band 4 (545-565 nm), 5 band (1230-1250 nm), band 6 (1628-1652 nm) and band 7 (2105-2155 nm). The bands used to calculate NDVI are: band 1 for red frequency and band 2 for near-infrared frequency. MOD09A1 provides georeferenced images with pixel resolution of 500m x 500m. This product has a mix of the best reflectance measures of each pixel in an 8-days period. The period of time selected on this study was from 2002 to 2017.

Daily data from a principal station of the meteorological network were utilized during the period studied (2002 – 2017). Meteorological station is located in 40°41'46"N 3°45'54"W (elevation 1004 m a.s.l.), less than 2 km from the study area (AEMET, 2017).

2.3 Site description

Six pixels (500m x 500m) are considered located in a pasture area at the north of the Community of Madrid (Spain) between the municipalities of “Soto del Real” and “Colmenar Viejo”. The study area is located between meridians 3° 45' 00" and 3° 47' 00" W and parallels 40° 42' 00" and 40° 44' 00" N approximately (see Fig. 1).

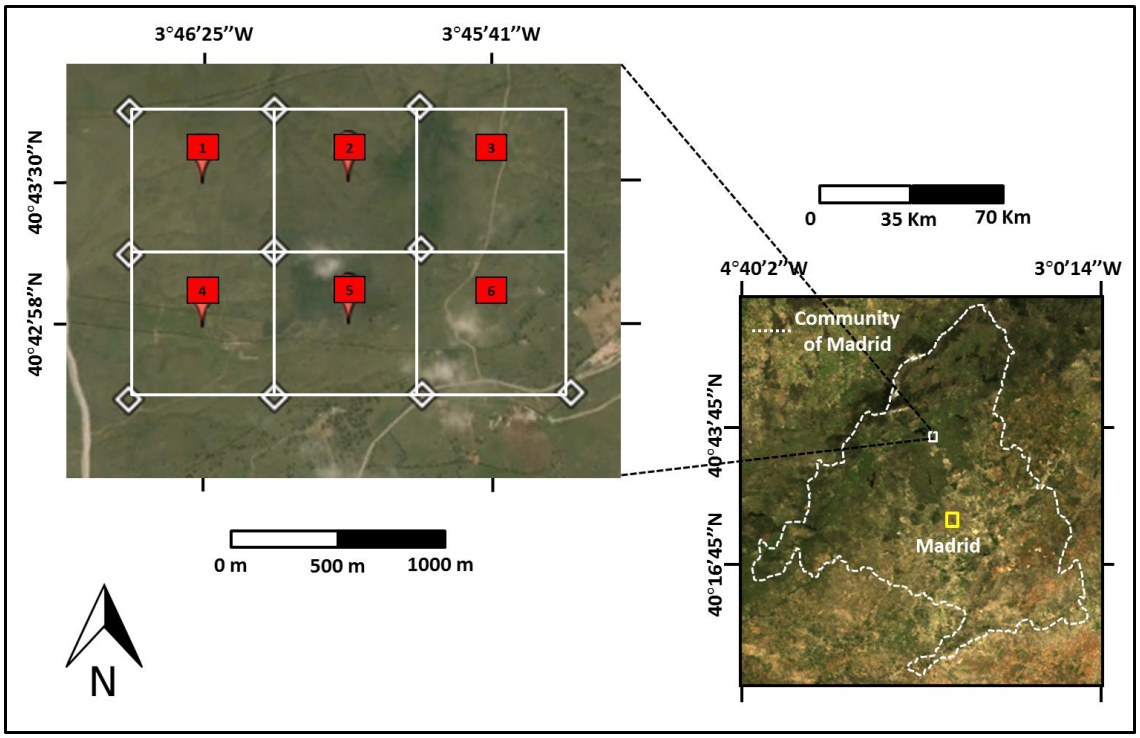

Figure 1. The study area is in the centre of the Iberian Peninsula (Community of Madrid). RGB image of six pixels area used for case study is shown (Google Earth´s and MODIS images).

The annual mean temperature ranges during the study period from 12.7°C to 13.8°C, and annual mean precipitation ranges from 360 mm to 781 mm. The stations studied were identified semi-arid (annual ratio P/ETo between 0.2 and 0.5) according to the global aridity index developed by the United-Nations Convention to Combat Desertification (UNEP, 1997). According to the climatic classification of Köppen (Kottek et al., 2006), this area presents a continental Mediterranean climate temperate with dry and temperate summer (type Csb). Temperature and precipitation of this site, based on 20 years, is presented in Table 1.

Due to high soil moisture conditions, ash is the dominant tree, forming large agroforestry systems ("dehesas") that are used for pasture. These are ecosystems with high biodiversity.

Table 1. Monthly average of maximum temperature (Tmax), average temperature (Tavg), minimum temperature (Tmin) and precipitation (P). Study period from 1997 to 2017.

Month	Jan	Feb	Mar	Apr	May	Jun	Jul	Aug	Sep	Oct	Nov	Dec	Annual
Tmax (ºC)	7.1	9.3	12.7	15.4	19.5	24.6	28.6	28.1	23.7	16.8	11.1	7.4	17.0
Tavg (ºC)	3.6	4.8	7.7	10.1	13.7	18.4	22.0	21.7	17.9	12.3	7.1	4.1	12.0

Tmin (ºC)	0.0	0.3	2.6	4.8	7.8	12.1	15.4	15.3	12.0	7.8	3.0	0.8	6.8
P (mm)	67.2	50.0	38.5	62.2	62.3	30.2	18.9	16.4	34.2	79.3	86.2	82.6	627.9

2.4 HSL model

There is no doubt that NDVI time-series from satellite sensors carry useful information, which can be used for characterizing seasonal dynamics of vegetation (Fensholt et al., 2012; Forkel et al., 2013). However, due to unfavorable atmospheric conditions during the data acquisition, NDVI time-series curve often contains noise (Motohka et al., 2011; Park, 2013). Although most of the NDVI data products are temporally composited through maximum value compositing (MVC) method (Holben, 1986) to retain relatively cloud-free data, residual noise still exists in the data, which will affect the accuracy of the NDVI value.

Therefore, usually it is necessary to reconstruct of NDVI time-series before extracting information from the noisy data. There are several techniques that have been applied to reduce noise and reconstruct NDVI series, a summary of these can be found in Wei et al. (2016). In this study we applied a simple filtering method based on the Hue-Saturation-Lightness (HSL) color model inspired by the work presented by Tackenberd (2007).

HSL color model is a cylindrical representation of RGB (Red-Green-Blue) points. Their components are Hue (color type), Saturation (level of color purity) and Lightness (color luminosity). Hue is the angular component and it is more intuitive for humans since it is directly related to the color wheel (see Fig. 2).

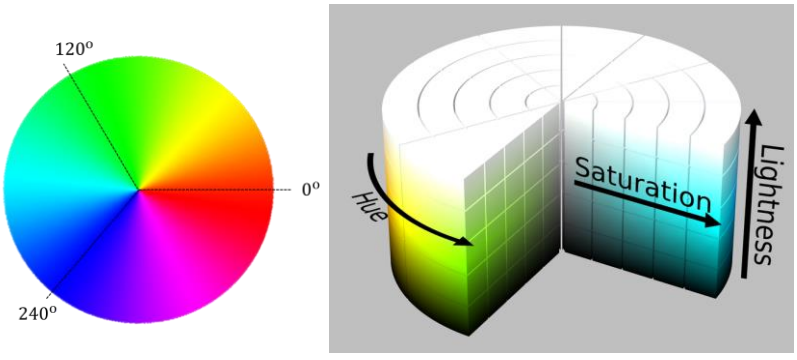

Figure 2. Colour wheel of Hue (on the left) and the HSL model (on the right).

Saturation is the radial component and near-zero values indicate grey colors. Lightness is the axial radial versus axial component, zero lightness produces black and full lightness produces white.

The NDVI series are filtered using the following HSL criterion: NDVI values are valid if HSL Saturation is greater than 0.15. In this way, the values of the series that have grey color correlate with pasture covered by clouds or snow are eliminated. This type of filter based in HSL color space has been used on digital camera images monitoring vegetation phenology (Tackenberg, 2007; Crimmins and Crimmins, 2008; Graham et al., 2009). However, we have not found the use of this HSL criterion in the context of NDVI remote sensing images.

2.5 Maximum Likelihood Method (MLM)

MLM estimates the set of parameters $\{\alpha, \beta, \mu, \sigma, \dots\}$ for a specific statistical distribution that maximizes the "likelihood function" or the "joint density function":

$$L = f(\boldsymbol{x}, \boldsymbol{\theta}) = \prod_{i=1}^{n} f(x_i; \alpha, \beta, \mu, \sigma, \dots) \quad (3)$$

where $\boldsymbol{x} = (x_1, \dots, x_n)$ is the set of data, $\boldsymbol{\theta} = (\alpha, \beta, \mu, \sigma, \dots)$ is the vector of parameters and $f(x_i; \alpha, \beta, \mu, \sigma, \dots)$ is the density function of the statistical model.

When maximization with respect to the vector of parameters is carried out, the estimated parameters $(\hat{\alpha}, \hat{\beta}, \hat{\mu}, \hat{\sigma}, \dots)$ for the proposed statistical distribution are obtained (Larson, 1982). Properties of estimated parameters are: invariance, consistency and asymptotically unbiased.

In the case of a Gaussian model, the estimated statistics μ and σ are defined by accurate expressions as follows:

$$\hat{\mu} = \bar{x} = \frac{1}{n}\sum_{i=1}^{n} x_i \qquad \hat{\sigma} = s = \sqrt{\frac{1}{n}\sum_{i=1}^{n}(x_i - \bar{x})^2} \quad (4)$$

where $\hat{\mu}$ is the sample mean and $\hat{\sigma}$ is the sample standard deviation of the data set.

In this study we will apply MLM to estimate the parameters for 4 probability density functions (PDF). In Table 2, a brief description is presented of these PDF candidates: Normal, Gamma, Beta and GEV. To do so, the following MATLAB functions have been used: "normfit", "gamfit", "betafit" and "gevfit" (respectively).

Table 2. Candidate Probability Density Functions (PDF).

PDF NAME	PDF EXPRESSION	PDF PARAMETERS

Normal	$\mathbf{f(x;\mu,\sigma)=\frac{1}{\sigma\sqrt{2\pi}}e^{-\frac{1}{2}\left(\frac{x-\mu}{\sigma}\right)^2}}$	$\boldsymbol{\mu \equiv average}$ $\boldsymbol{\sigma \equiv standard\ deviation}$
Gamma	$\mathbf{f(x;\alpha,\beta)=\frac{1}{\beta^{\alpha}\Gamma(\alpha)}x^{\alpha-1}e^{-\frac{x}{\beta}}}$	$\boldsymbol{\Gamma(.) \equiv gamma\ function}$ $\boldsymbol{\alpha}$ *and* $\boldsymbol{\beta \equiv parameters}$
Beta	$\mathbf{f(x;a,b)=\frac{\Gamma(a+b)}{\Gamma(a)\Gamma(a)}x^{a-1}(1-x)^{b-1}}$	$\boldsymbol{\Gamma(.) \equiv gamma\ function}$ $\boldsymbol{a}$ *and* $\boldsymbol{b \equiv parameters}$
GEV	$\mathbf{f(x;\mu,\sigma,\xi)=\frac{1}{\sigma}t(x)^{\xi+1}e^{-t(x)}}$ where $\mathbf{t(x)}=\begin{cases}\left(1+\left(\frac{x-\mu}{\sigma}\right)\xi\right)^{-1/\xi} & \text{if } \xi\neq 0\\ e^{-(x-\mu)/\sigma} & \text{if } \xi=0\end{cases}$	$\boldsymbol{\mu \in \mathbb{R} \equiv location\ param.}$ $\boldsymbol{\sigma > 0 \equiv scale\ parameter}$ $\boldsymbol{\xi \in \mathbb{R} \equiv shape\ parameter}$

2.6 Goodness of fit (Chi-square test)

χ^2 test can be used to determine to what extent observed frequencies differ from frequencies expected for a specific statistical model. The most important points of the theory are briefly presented in (Cochran, 1952).

Let $f(x,\theta)$ be a theoretical density function of a random variable X which depends on parameters $\theta=(\alpha,\beta,\mu,\sigma,\dots)$ and let $x_1,\dots,x_n$ be a sample of X grouped into k classes with n_i data per class i.

Firstly, the following hypothesis is set:

(H_0) observed data fit theoretical distribution $f(x,\theta)$.

Then the test statistic χ_c^2 is defined as:

$$\chi_c^2=\sum_{i=0}^{k}\frac{(n_i-e_i)^2}{e_i} \tag{5}$$

where n_i is the number of data or observed frequency and $e_i=n\cdot P(class\ i)$ is the expected frequency for class i. $P(class\ i)$ is the theoretical interval probability defined for class i.

A level of significance is also set as:

$$\alpha=P(RejectH_0\ /\ H_0 is\ true\ ) \tag{6}$$

Finally, the following decision rule is applied: "reject the theoretical distribution at significance level α if:

$$\chi_c^2>\chi^2_{(k-m-1,1-\alpha)} \tag{7}$$

where $\chi^2_{(k-m-1,1-\alpha)}$ is a χ^2 distribution with k-m-1 degrees of freedom (m is the number of parameters, k is the number of classes).

3. Results and Discussion

3.1 HSL filtering criterion

NDVI series (from 2002 to 2017) were obtained for each pixel of the study area using frequency bands provided by MODIS product named MOD09A1. These series contain some irregular values that can skew NDVI pattern. Therefore, the six series (six pixels) were filtered using the HSL criterion. In Fig. 3 is shown an example of how HSL filtering criterion works with a 10 years NDVI series (from 2002 to 2012).

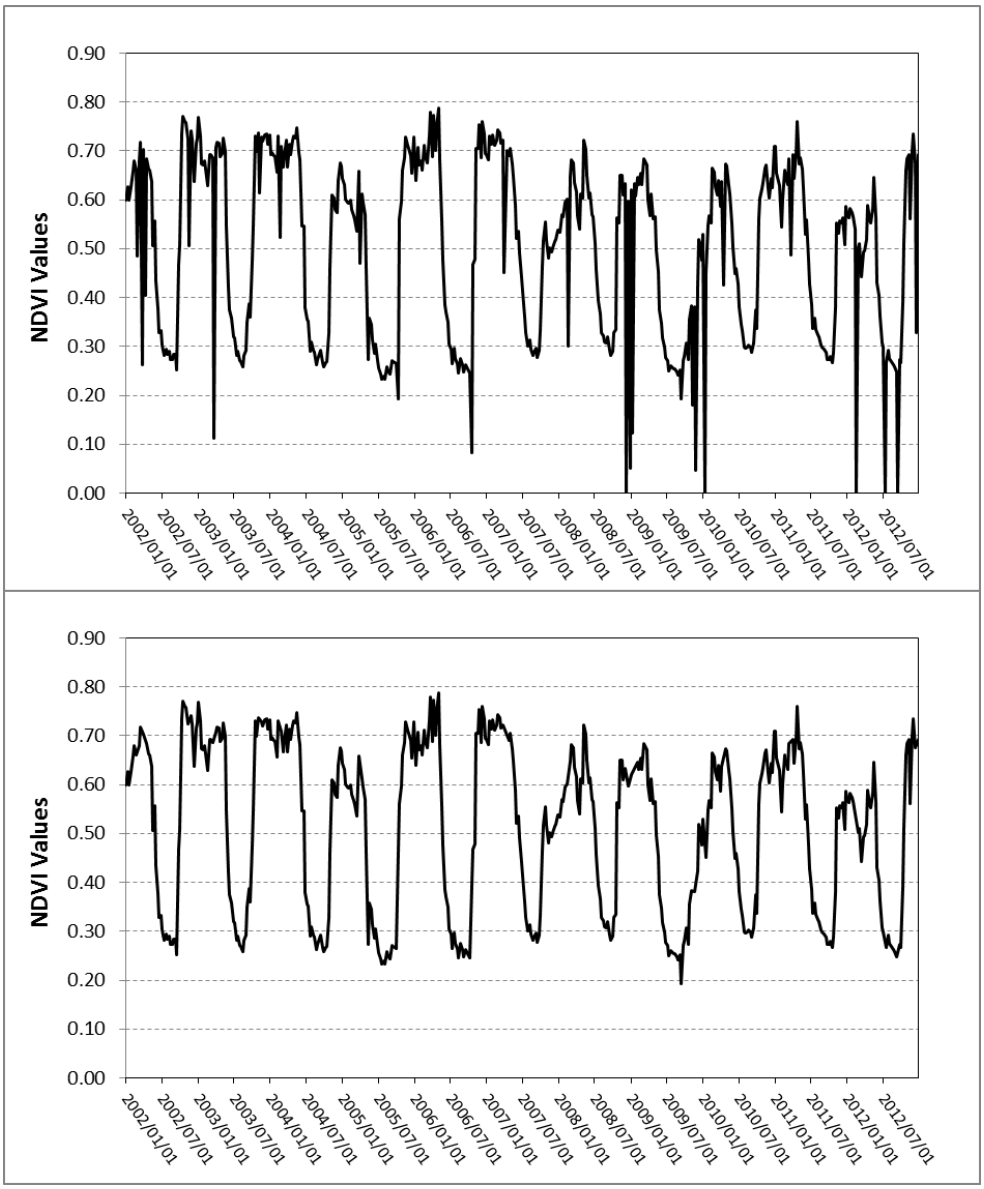

Figure 3. HSL filtering criterion applied to a 10 years NDVI series. Top graph shows the real NDVI series. Bottom graph shows the HSL filtered NDVI series.

The abrupt changes in the NDVI values, mainly observed during raining seasons such as autumn and winter, are efficiently eliminated. Not to be a high computational demanding method is one of the main advantages of HSL filtering method. Therefore, this method will allow us to obtain more robust NDVI values to be used in the statistical analysis.

3.2 Maximum Likelihood Method (MLM) and Chi square test

NDVI values were obtained consecutively every 8 days from MODIS product starting at 1st of January of every year, in such a way that 46 NDVI observations were considered for each year. Therefore, 46 Random Variables (RV) were defined when taking into account all the years of this study.

In Table 3, every RV (named as "Interval") can be seen together with the number of available NDVI observations. Each RV collects the observations coming from the six selected pixels. The start intervals of each season are: interval 45 for winter, interval 11 for spring, interval 23 for summer and interval 34 for autumn.

Table 3. Number of observations for every RV (named as Interval).

RANDOM VARIABLE	# OBSERVATIONS	RANDOM VARIABLE	# OBSERVATIONS
Interval 1	85	**Interval 24**	96
Interval 2	84	**Interval 25**	96
Interval 3	96	**Interval 26**	96
Interval 4	96	**Interval 27**	96
Interval 5	95	**Interval 28**	96
Interval 6	90	**Interval 29**	96
Interval 7	86	**Interval 30**	96
Interval 8	83	**Interval 31**	96
Interval 9	96	**Interval 32**	96
Interval 10	96	**Interval 33**	94
Interval 11	74	**Interval 34**	96
Interval 12	88	**Interval 35**	96
Interval 13	88	**Interval 36**	85
Interval 14	88	**Interval 37**	90
Interval 15	96	**Interval 38**	96
Interval 16	92	**Interval 39**	92
Interval 17	88	**Interval 40**	90
Interval 18	96	**Interval 41**	96
Interval 19	95	**Interval 42**	89
Interval 20	96	**Interval 43**	95
Interval 21	95	**Interval 44**	88
Interval 22	96	**Interval 45**	90
Interval 23	96	**Interval 46**	90

In Fig. 4, a plot with NDVI sample means of all RV with a start and end reference of the astronomical seasons is shown. The typical evolution of the NDVI along a year can be seen.

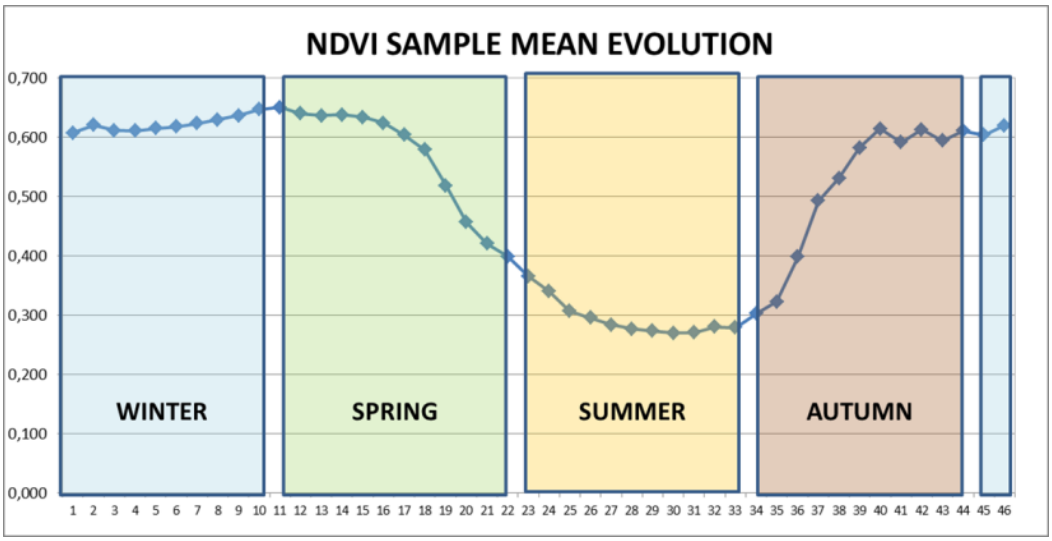

Figure 4. NDVI sample means of 46 random variables (RV) are shown as well as start and end reference of every season. Study period from 2002 to 2017.

The observed evolution of NDVI through the different seasons is typical of the pasture in this area. The summer presents the lowest mean values which begin to increase in autumn achieving a maximum mean value of 0.60 or 0.65 during winter. In the middle of the spring NDVI decrease again, approaching the lowest mean value of 0.28 approximately.

Taking into account these values, dense vegetation, in this study pasture, is found from middle of October (interval 37) till the end of May (interval 19). It is in this period where the precipitation concentrates (see Table 1). During the summer, the NDVI mean values are lower than 0.3 corresponding with low precipitation and high temperatures.

Following the work of Escribano-Rodriguez et al. (2014), there is a relationship of pasture damage and a NDVI value around 0.40. Even if the authors point out that this value is highly variable depending on the location, we can see that summer season in this case study is under this value (see Fig. 4). This can explain that “Insurances for Damaged Pasture” usually do not apply in these dates due to the arid environment (BOE, 2013).

MLM has been applied to model these 46 RV. Parameters have been calculated for 4 PDF (see Table 2) which are the candidates to be the best fit. To check the goodness of the

fit of PDF candidates, Chi square test (χ^2 test) has been used from 7 classes to 14 classes meeting the requirement that each class has at least five observations. The level of significance (α) was fixed to 5% for all the candidates.

Twelve intervals (from 23 to 34) corresponding to months of July, August and September have been excluded of this analysis since these intervals fall into the dry season in the study area, normally not cover by any SIBI. Therefore, calculations were carried out over 34 intervals. Fig. 5 shows the percentage of intervals that fit for every PDF candidate. The number of classes used in χ^2 test is represented at X-axis (from 7 to 14 classes).

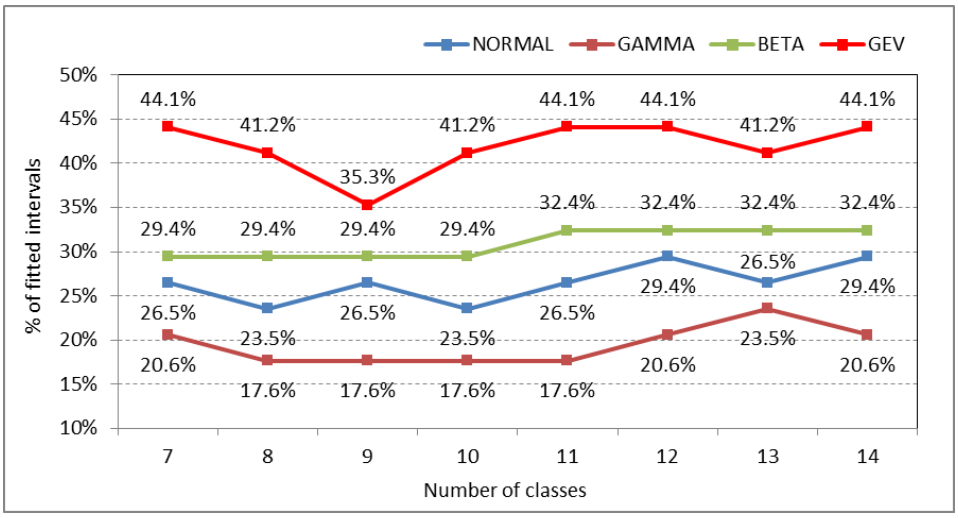

Figure 5. Percentage of fitted intervals (Y axis) for each PDF candidate (Normal, Gamma, Beta and GEV distributions) in function of the number of classes (X axis).

Fig. 5 indicates that GEV distributions explain more intervals (more than 40% for the majority of the class analysis) than Normal, Gamma or Beta distributions. An important difference between the Normal distribution and the rest of the PDF used in this work is its symmetry and kurtosis. Many of the observed NDVI distributions present a clear asymmetry and long tails in one or both sides that causes Normal distribution not to be the optimal fit.

There is a relationship between seasons and the number of intervals that fit correctly. We found that GEV distributions explain better some intervals of spring and autumn since their observed distributions are very asymmetric. On the other hand, we did not find an important difference in winter, since its observed distributions are mainly symmetric.

Therefore, the methodology using the NDVI Normal assumption applied to design an index-based insurance will not be feasible in many intervals of this study.

Table A1 at Appendix A shows the estimated parameters for each PDF and each interval calculated by the MLM. These parameters were used to compare the estimated PDF with the NDVI observed values on different times through the seasons. The following intervals are shown as examples of better GEV fit: interval 4 and 8 (for winter, see Fig. 6), interval 17 and 21 (for spring, see Fig. 7) and interval 36 and 40 (for autumn, see Fig. 8). In these plots, observed frequency is compared versus Normal and GEV density distributions calculated by MLM.

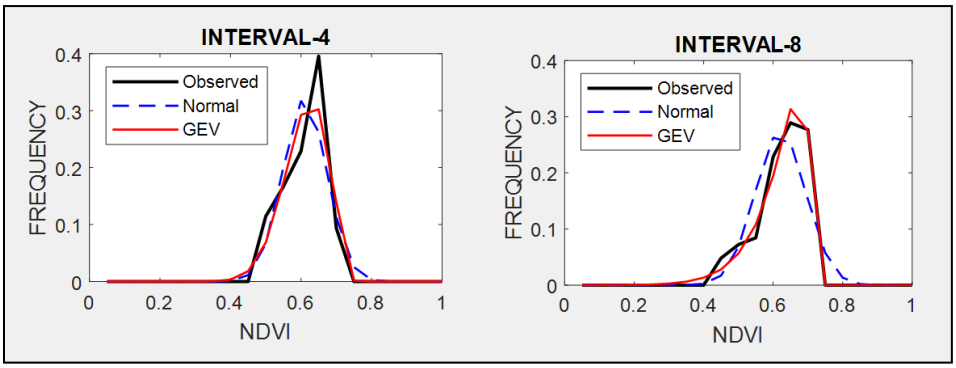

Figure 6. Comparison between observed NDVI frequency, GEV and Normal probability density functions (PDF) on two different dates. Intervals 4 and 8 are examples for winter.

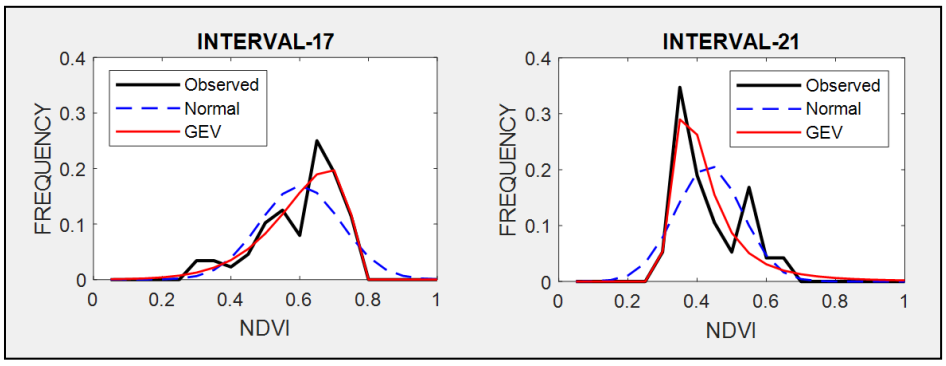

Figure 7. Comparison between observed NDVI frequency, GEV and Normal probability density functions (PDF) on two different dates. Intervals 17 and 21 are examples for spring.

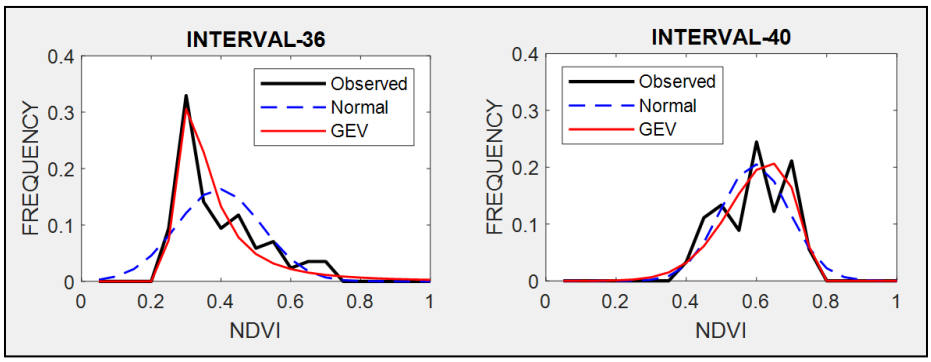

Figure 8. Comparison between observed NDVI frequency, GEV and Normal probability density functions (PDF) on two different times. Intervals 36 and 41 are examples for autumn.

During winter (see Fig. 6) the observed NDVI distribution presents negative skewness. Then, there is a higher frequency of high NDVI values corresponding with significant precipitation. During spring an evolution in the skewness is observed passing from negative to positive, and so, the lower NDVI values become the higher probable. Finally, during autumn precipitation begins and from positive pass to negative skewness and higher NDVI values are possible. We can observe that Normal distribution has no flexibility to follow this dynamic in the distributions on each time. This comparison is done in a sequential order for the whole of intervals in Figures A1, A2, A3 and A4 at Appendix A.

The more skewness and kurtosis depart from those of the Normal distribution the larger the errors affecting the insurance designed based on (Turvey et al., 2012). It is an expected result as pasture scenario is quite different from the development of a crop, where Normal distributions in the NDVI values are more expected. This high heterogeneity in time and space of NDVI estimated on pasture has been pointed out in several works (Martin-Sotoca et al, 2018). At the same time, more different is the observed NDVI frequency from a Normal distribution less representative is the average, and so, the median becomes a more representative value.

3.3 Insurance context

The use of NDVI thresholds in damaged pasture context was presented in the introduction section, being an example of using the "Insurance for Damaged Pasture" in Spain. We have chosen this last insurance to compare the results between applying Normal and GEV distribution methodologies. In this particular case the NDVI threshold ($NDVI_{th}$) was calculated using the expression $NDVI_{th} = \mu - k \cdot \sigma$ (where μ, σ are average and standard deviation of NDVI distributions respectively, assuming the Normal hypothesis).

The probability of being below $NDVI_{th}$ (using $k = 0.7$, first damage level in the insurance) at every interval has been calculated assuming the Normal hypothesis. As it was expected, this value is always 24.2% (see third column in Table 4). The probability of being below $NDVI_{th}$ has also been calculated using GEV distributions obtained in this study. The probability obtained by GEV distributions is mostly lower than the Normal distributions in spring, autumn and winter (see Table 4) that is the working period of the insurance.

Observing where in time are localized the highest relative error in probabilities (fifth column in Table 4), in absolute values, intervals corresponding to the end of winter, second middle of spring and the beginning of autumn present errors higher than 10%. This could explain why it is in spring and autumn when more disagreements exist between farmers and insurance company in claims.

Table 4 – First column: time intervals of approximately 8 days along the year. **Second column:** NDVI thresholds ($NDVI_{th}$) based on a Normal distribution applying $\mu - 0.7 \times \sigma$. **Third column:** percentages of area below the $NDVI_{th}$ when Normal distributions are applied. **Fourth column:** percentages of area below the $NDVI_{th}$ when GEV distributions are applied. **Fifth column:** relative area error of GEV compared to the Normal distribution.

RANDOM VARIABLE	NORMAL		GEV	
	$NDVI_{th}$	Prob.	Prob.	Error (%)
Interval 1	0.535	24.20%	24.37%	0.70%
Interval 2	0.541	24.20%	23.18%	-4.21%
Interval 3	0.541	24.20%	23.27%	-3.84%
Interval 4	0.543	24.20%	23.27%	-3.84%
Interval 5	0.545	24.20%	24.17%	-0.12%
Interval 6	0.534	24.20%	21.48%	-11.24%
Interval 7	0.528	24.20%	24.01%	-0.79%
Interval 8	0.546	24.20%	20.70%	-14.46%
Interval 9	0.555	24.20%	21.30%	-11.98%
Interval 10	0.561	24.20%	22.28%	-7.93%
Interval 11	0.567	24.20%	23.49%	-2.93%
Interval 12	0.572	24.20%	23.75%	-1.86%
Interval 13	0.571	24.20%	23.20%	-4.13%
Interval 14	0.570	24.20%	24.29%	0.37%
Interval 15	0.571	24.20%	23.47%	-3.02%

Interval 16	0.560	24.20%	23.26%	-3.88%
Interval 17	0.495	24.20%	21.29%	-12.02%
Interval 18	0.484	24.20%	21.58%	-10.83%
Interval 19	0.442	24.20%	23.06%	-4.71%
Interval 20	0.381	24.20%	27.20%	12.40%
Interval 21	0.342	24.20%	29.46%	21.74%
Interval 22	0.323	24.20%	28.84%	19.17%
Interval 35	0.257	24.20%	18.98%	-21.57%
Interval 36	0.285	24.20%	28.57%	18.06%
Interval 37	0.333	24.20%	25.90%	7.02%
Interval 38	0.398	24.20%	24.27%	0.29%
Interval 39	0.454	24.20%	23.79%	-1.69%
Interval 40	0.503	24.20%	22.81%	-5.74%
Interval 41	0.491	24.20%	23.23%	-4.01%
Interval 42	0.517	24.20%	24.66%	1.90%
Interval 43	0.507	24.20%	23.13%	-4.42%
Interval 44	0.514	24.20%	23.49%	-2.93%
Interval 45	0.515	24.20%	23.70%	-2.07%
Interval 46	0.509	24.20%	23.33%	-3.60%

In Table 4, Normal $\boldsymbol{NDVI_{th}}$ have been used to calculate the probability in GEV distributions. An alternative calculation can be the use of Normal probability (24.2%) to calculate new $\boldsymbol{NDVI_{th}}$ based on GEV (see Table 5). It can be seen that new $\boldsymbol{NDVI_{th}}$ obtained by GEV distributions are mostly upper than thresholds using Normal distributions in spring, autumn and winter. Considering these results we find that damage thresholds calculated by GEV methodology are mostly above that one's calculated by Normal methodology.

Again, intervals corresponding to the end of winter, second middle of spring and the beginning of autumn present $\boldsymbol{NDVI_{th}}$ relative errors higher than 1% in absolute values (fourth column in Table 5).

Table 5 - First column: time intervals of approximately 8 days along the year. **Second column:** NDVI thresholds ($NDVI_{Th}$) based on a Normal distribution (Normal) applying $\mu - 0.7 \times \sigma$. **Third column:** $NDVI_{Th}$ based on a GEV distribution (GEV) using 24.2% as the area below the $NDVI_{Th}$. **Fourth column:** relative $NDVI_{Th}$ error of GEV compared to the Normal distribution.

RANDOM VARIABLE	$NDVI_{Th}$		
	Normal	GEV	Error (%)
Interval 1	0.535	0.534	-0,19%
Interval 2	0.541	0.543	0,37%
Interval 3	0.541	0.543	0,37%
Interval 4	0.543	0.545	0,37%
Interval 5	0.545	0.545	0,00%
Interval 6	0.534	0.543	1,69%
Interval 7	0.528	0.528	0,00%
Interval 8	0.546	0.558	2,20%
Interval 9	0.555	0.563	1,44%
Interval 10	0.561	0.567	1,07%
Interval 11	0.567	0.569	0,35%
Interval 12	0.572	0.574	0,35%
Interval 13	0.571	0.574	0,53%
Interval 14	0.570	0.569	-0,18%
Interval 15	0.571	0.573	0,35%
Interval 16	0.560	0.563	0,54%
Interval 17	0.495	0.510	3,03%
Interval 18	0.484	0.498	2,89%
Interval 19	0.442	0.447	1,13%
Interval 20	0.381	0.374	-1,84%
Interval 21	0.342	0.334	-2,34%
Interval 22	0.323	0.318	-1,55%
Interval 35	0.257	0.262	1,95%
Interval 36	0.285	0.278	-2,46%
Interval 37	0.333	0.327	-1,80%
Interval 38	0.398	0.398	0,00%
Interval 39	0.454	0.455	0,22%
Interval 40	0.503	0.508	0,99%
Interval 41	0.491	0.494	0,61%
Interval 42	0.517	0.516	-0,19%
Interval 43	0.507	0.510	0,59%
Interval 44	0.514	0.516	0,39%
Interval 45	0.515	0.516	0,19%
Interval 46	0.509	0.511	0,39%

549

550

551 **4. Conclusions**

According to the results obtained in the study area using MLM and χ^2 test, it can be concluded that Normal distributions are not the best fit to the NDVI observations, and GEV distributions provide a better approximation.

The difference between Normal and GEV assumption is more evident in the transition from winter to summer (spring), where NDVI values decrease, and then from summer to winter (autumn) presenting the opposite behavior of increasing NDVI values. In both periods asymmetrical distributions were found, negative skewness for the spring transition and positive skewness for the autumn transition. During both periods the variability in precipitation and temperatures were higher in this location.

We have found differences if GEV assumption is selected instead of the Normal one when defining damaged pasture thresholds ($NDVI_{th}$). The use of these different assumptions should be taken into account in future insurance implementations due to the important consequences of supposing a damage event or not. We propose the use of quantiles in observed NDVI distributions instead of average and standard deviation, typically of Normal distributions, to calculate new $NDVI_{th}$.

Acknowledgements

This research has been partially supported by funding from MINECO under contract No. MTM2015-63914-P and CICYT PCIN-2014-080.

Appendix A

Table A1 - Maximum Likelihood parameters calculated for 4 PDF.

RANDOM VARIABLE	NORMAL		GAMMA		BETA		GEV		
	μ	σ	α	β	a	b	μ	σ	ξ
Interval 1	0.591	0.081	53.31	0.011	21.45	14.82	0.563	0.080	-0.297
Interval 2	0.589	0.069	71.14	0.008	30.62	21.40	0.571	0.073	-0.477
Interval 3	0.583	0.060	94.15	0.006	39.56	28.34	0.567	0.063	-0.457
Interval 4	0.585	0.060	91.88	0.006	39.58	28.05	0.570	0.064	-0.468
Interval 5	0.588	0.061	93.92	0.006	38.83	27.25	0.568	0.061	-0.340
Interval 6	0.582	0.068	70.28	0.008	30.67	22.05	0.577	0.083	-0.846
Interval 7	0.584	0.080	52.52	0.011	22.16	15.82	0.559	0.082	-0.366
Interval 8	0.596	0.071	65.37	0.009	28.89	19.59	0.591	0.081	-0.833
Interval 9	0.601	0.066	76.02	0.008	34.31	22.84	0.590	0.070	-0.652
Interval 10	0.613	0.073	63.83	0.010	27.80	17.62	0.598	0.079	-0.572
Interval 11	0.621	0.078	58.72	0.011	24.33	14.86	0.600	0.083	-0.451
Interval 12	0.624	0.073	68.33	0.009	28.01	16.94	0.603	0.078	-0.431
Interval 13	0.624	0.075	66.22	0.009	26.23	15.85	0.604	0.080	-0.476
Interval 14	0.631	0.088	50.23	0.013	18.71	10.92	0.603	0.090	-0.342
Interval 15	0.630	0.084	53.60	0.012	21.17	12.45	0.607	0.089	-0.448
Interval 16	0.627	0.096	38.75	0.016	16.08	9.59	0.602	0.103	-0.474
Interval 17	0.577	0.117	20.47	0.028	10.24	7.58	0.560	0.127	-0.692
Interval 18	0.568	0.120	20.52	0.028	9.71	7.42	0.552	0.136	-0.718
Interval 19	0.523	0.116	19.46	0.027	9.52	8.68	0.495	0.125	-0.493
Interval 20	0.452	0.101	20.99	0.022	10.98	13.31	0.401	0.077	0.078
Interval 21	0.409	0.095	19.94	0.021	11.18	16.13	0.354	0.060	0.325
Interval 22	0.379	0.080	24.66	0.015	14.41	23.52	0.333	0.046	0.385
Interval 23	0.353	0.073	26.54	0.013	15.85	29.01	0.311	0.036	0.456
Interval 24	0.328	0.056	38.36	0.009	24.22	49.65	0.298	0.033	0.287
Interval 25	0.305	0.044	53.52	0.006	35.62	81.20	0.282	0.028	0.210
Interval 26	0.298	0.034	78.93	0.004	54.47	128.55	0.283	0.029	-0.064
Interval 27	0.289	0.026	126.85	0.002	88.33	217.15	0.278	0.021	-0.030
Interval 28	0.282	0.022	166.17	0.002	119.50	305.03	0.274	0.022	-0.322
Interval 29	0.278	0.021	179.09	0.002	127.93	332.63	0.269	0.018	-0.085
Interval 30	0.273	0.019	203.11	0.001	147.67	393.21	0.266	0.019	-0.247
Interval 31	0.272	0.022	166.83	0.002	120.11	321.95	0.262	0.018	-0.059
Interval 32	0.280	0.034	75.63	0.004	52.36	134.30	0.264	0.023	0.118
Interval 33	0.285	0.034	82.05	0.004	54.90	137.68	0.270	0.020	0.122
Interval 34	0.295	0.057	33.26	0.009	21.15	50.37	0.268	0.024	0.363

Interval 35	0.312	0.079	19.70	0.016	11.83	25.94	0.275	0.038	0.300
Interval 36	0.369	0.121	10.81	0.034	6.11	10.33	0.298	0.063	0.480
Interval 37	0.432	0.141	9.45	0.046	5.21	6.81	0.370	0.120	-0.080
Interval 38	0.487	0.128	13.88	0.035	7.25	7.63	0.445	0.127	-0.321
Interval 39	0.529	0.107	23.56	0.022	11.39	10.16	0.497	0.110	-0.390
Interval 40	0.570	0.096	34.02	0.017	15.10	11.40	0.548	0.105	-0.533
Interval 41	0.554	0.090	36.42	0.015	16.90	13.64	0.531	0.096	-0.471
Interval 42	0.583	0.095	37.29	0.016	15.56	11.11	0.551	0.094	-0.295
Interval 43	0.574	0.097	34.27	0.017	14.93	11.07	0.550	0.103	-0.482
Interval 44	0.572	0.083	47.13	0.012	20.40	15.26	0.549	0.086	-0.425
Interval 45	0.576	0.088	42.59	0.014	18.17	13.36	0.550	0.090	-0.396
Interval 46	0.570	0.088	41.98	0.014	18.11	13.66	0.546	0.092	-0.445

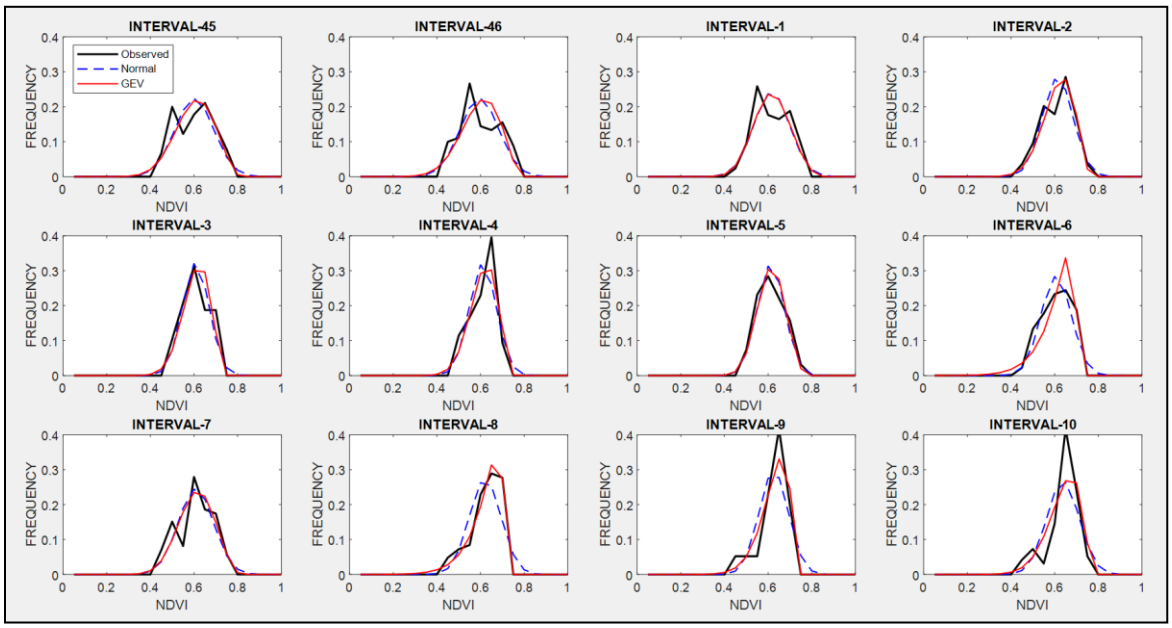

Figure A1. Observed NDVI, GEV and Normal probability density functions (PDF) from interval 45 to interval 10 (from 19 December to 21 March) representing winter.

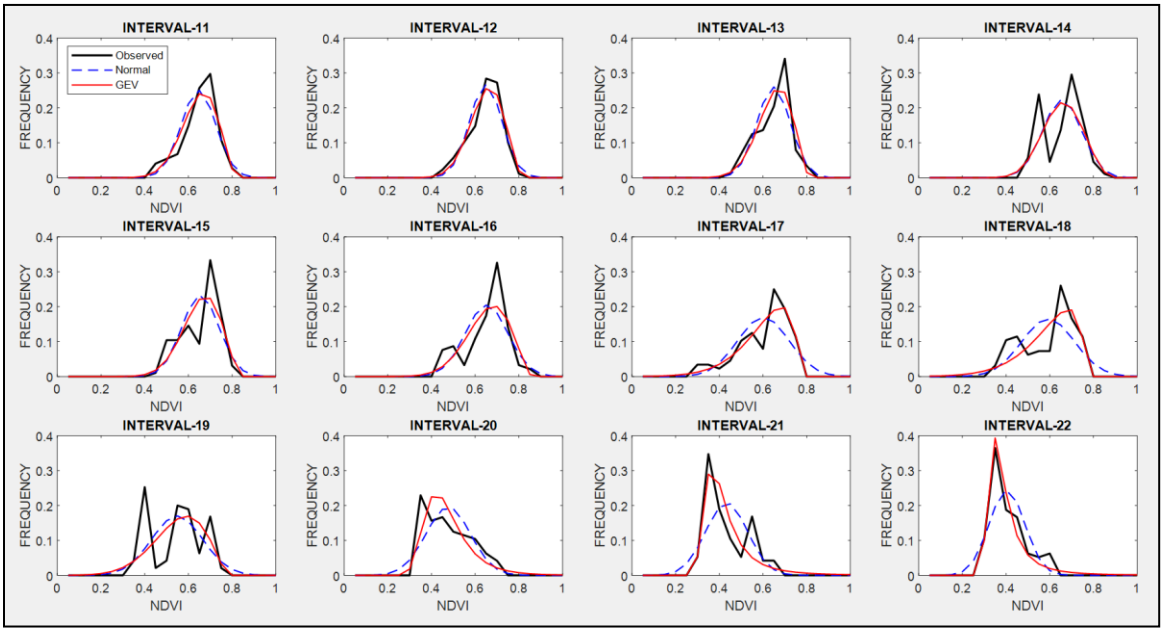

586

587 **Figure A2.** Observed NDVI, GEV and Normal probability density functions (PDF) from interval 11 to
588 interval 22 (from 22 March to 25 June) representing spring.

589

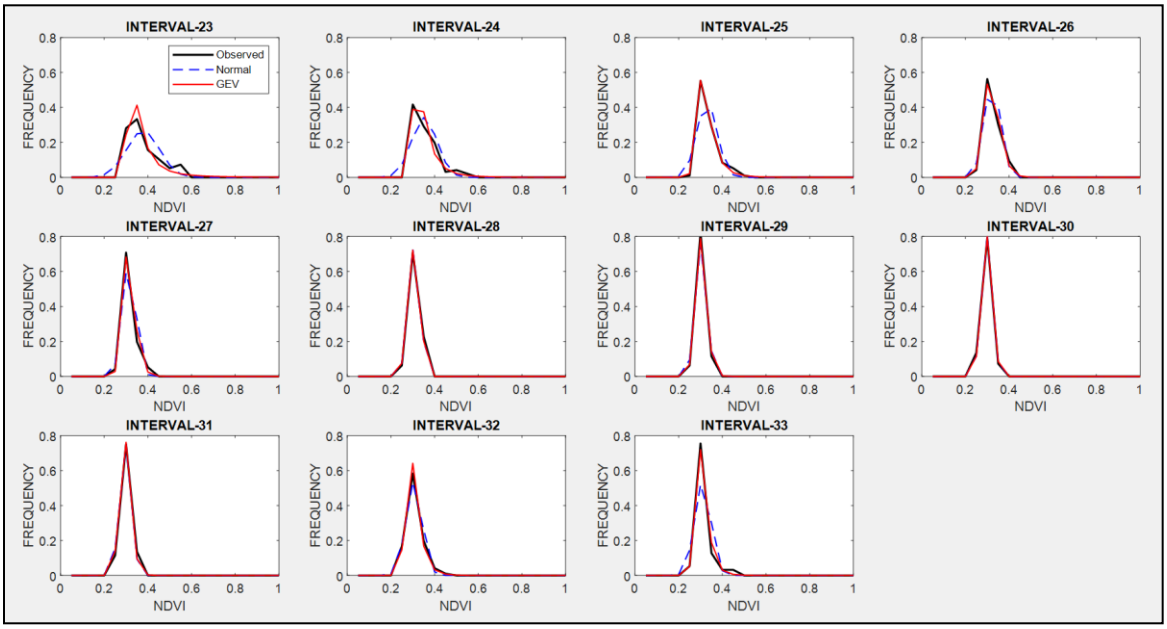

590

591 **Figure A3.** Observed NDVI, GEV and Normal probability density functions (PDFs) from interval 23
592 to interval 33 (from 26 June to 21 September) representing summer.

593

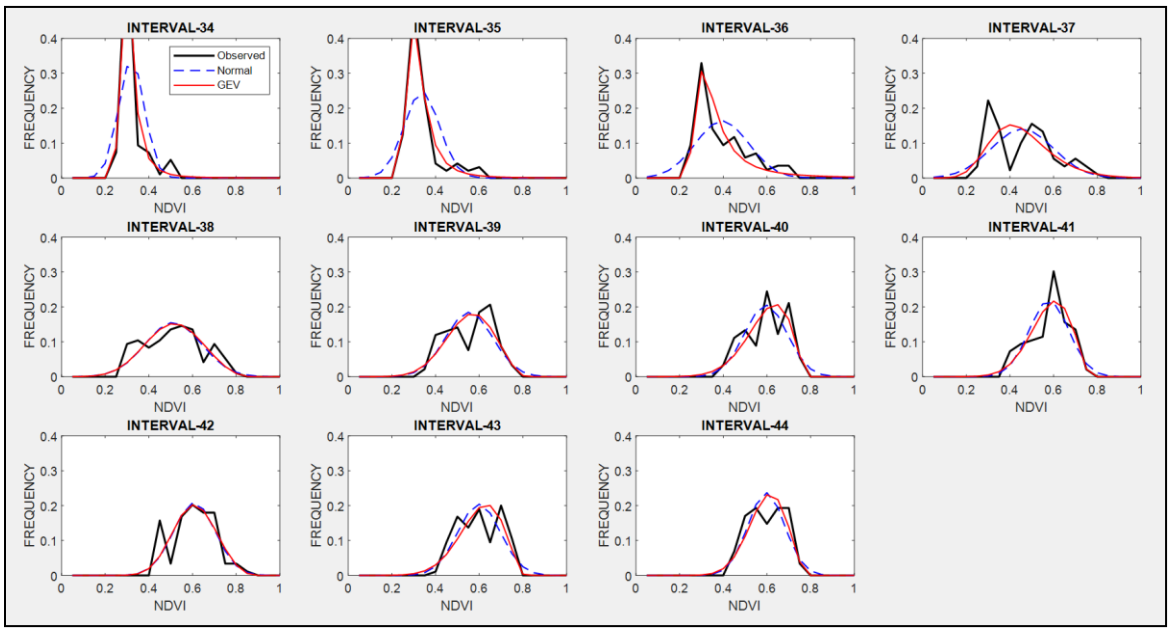

Figure A4. Observed NDVI, GEV and Normal PDFs from interval 34 to interval 44 (from 22 September to 18 December) representing autumn.

References

Agencia Estatal de Meteorología (AEMET). Available at: www.aemet.es, 2017.

Al-Bakri, J. T., and Taylor, J. C.: Application of NOAA AVHRR for monitoring vegetation conditions and biomass in Jordan, J. Arid Environ, 54, 579–593, 2003.

Bailey, S.: The Impact of Cash Transfers on Food Consumption in Humanitarian Settings: A review of evidence, Study for the Canadian Foodgrains Bank, May 2013.

Boletin Oficial del Estado (BOE, 6638 - Orden AAA/1129/2013. Nº 145, III, p-46077, 2013.

Cochran, William G.: The Chi-square Test of Goodness of Fit, Annals of Mathematical Statistics. 23: 315–345, 1952.

Crimmins, M. A., and Crimmins T. M.: Monitoring plant phenology using digital repeat photography, Environ. Manage, 41, 949-958, 2008.

Dalezios, N. R., Blanta, A., Spyropoulos, N. V., and Tarquis A. M.: Risk identification of agricultural drought for sustainable Agroecosystems, Nat. Hazards Earth Syst. Sci., 14, 2435–2448, 2014.

Dalezios, N. R.: The Role of Remotely Sensed Vegetation Indices in Contemporary Agrometeorology. Invited paper in Honorary Special Volume in memory of late Prof. A. Flokas. Publisher: Hellenic Meteorological Association, 33-44, 2013.

De Leeuw, J., Vrieling, A., Shee, A., Atzberger, C., Hadgu, K. M., Biradar, C. M., Humphrey Keah, H., and Turvey, C.: The Potential and Uptake of Remote Sensing in Insurance: A Review, Remote Sens., 6(11), 10888-10912, 2014.

Escribano Rodríguez, J. Agustín, Díaz-Ambrona, Carlos Gregorio H., and Tarquis Alfonso, Ana María: Selection of vegetation indices to estimate pasture production in Dehesas, PASTOS, 44(2), 6-18, 2014.

Fensholt, R., and Proud, S. R.: Evaluation of earth observation based global long term vegetation trends - comparing GIMMS and MODIS global NDVI time series, Remote Sens. Environ., 119, 131–147, 2012.

Flynn E. S.: Using NDVI as a pasture management tool. Master Thesis, University of Kentucky, 2006.

Forkel, M., Carvalhais, N., Verbesselt, J., Mahecha, M.D., Neigh, C. S., and Reichstein, M.: Trend change detection in NDVI time series: effects of inter-annual variability and methodology, Remote Sens., 5, pp, 2113–2144, 2013.

Fuller, D.O.: Trends in NDVI time series and their relation to rangeland and crop production in Senegal, 1987–1993, Int. J. Remote Sens., 19, 2013–2018, 1998.

Gommes, R., and Kayitakire, F.: The challenges of index-based insurance for food security in developing countries. Proceedings, Technical Workshop, JRC, Ispra, 2-3 May 2012. Publisher: JRC-EC, p. 276, 2013.

635 Gouveia, C., Trigo, R. M., and Da Camara, C. C.: Drought and vegetation stress monitoring
636 in Portugal using satellite data, Nat. Hazards Earth Syst. Sci., 9, 185-195, 2009.
637 Goward, S. N., Tucker, C. J., and Dye, D.G.: North-American vegetation patterns observed
638 with the NOAA-7 advanced very high-resolution radiometer. Vegetation, 64, 3–14,
639 1985.
640 Graham, E. A., Yuen, E. M., Robertson, G. F., Kaiser, W. J., Hamilton, M. P., and Rundel, P.
641 W.: Budburst and leaf area expansion measured with a novel mobile camera system
642 and simple color thresholding, Environ. Exp. Bot., 65, 238-244, 2009.
643 Hobbs, T. J.: The use of NOAA-AVHRR NDVI data to assess herbage production in the arid
644 rangelands of central Australia, Int. J. Remote Sens., 16, 1289–1302, 1995.
645 Holben, B. N.: Characteristics of maximum-value composite images from temporal AVHRR
646 data, Int. J. Remote Sens., 7, 1417–1434, 1986.
647 Kottek, M., Grieser, J., Beck, C., Rudolf, B., and Rubel, F.: World Map of the Köppen-Geiger
648 climate classification updated, Meteorologische Zeitschrift, 15, 259-263, 2006.
649 Kundu, A., Dwivedi, S., and Dutta, D.: Monitoring the vegetation health over India during
650 contrasting monsoon years using satellite remote sensing indices, Arab J Geosci., 9,
651 144, 2016.
652 Land Processes Distributed Active Archive Center (LP DAAC): Surface Reflectance 8-Day L3
653 Global 500m. NASA and USGS. Available at:
654 https://lpdaac.usgs.gov/products/modis_products_Table/mod09a1. 2014.
655 Larson, H. J.: Introduction to Probability Theory and Statistical Inference (3rd edition). New
656 York, John Wiley and Sons, 1982.
657 Leblois, A.: Weather index-based insurance in a cash crop regulated sector: ex ante
658 evaluation for cotton producers in Cameroon. Paper presented at the JRC/IRI
659 workshop on The Challenges of Index-Based Insurance for Food Security in Developing
660 Countries, Ispra, 2-3, May, 2012.
661 Lovejoy, S., Tarquis, A. M., Gaonac'h, H., and Schertzer, D.: Single and Multiscale remote
662 sensing techniques, multifractals and MODIS derived vegetation and soil moisture.
663 Vadose Zone J., 7, 533-546, 2008.
664 Maples, J. G., Brorsen, B. W., and Biermaches, J. T.: The rainfall Index Annual Forage pilot
665 program as a risk management tool for cool-season forage. J. Agr. Appl Econ, 48(1),
666 29–51, 2016.
667 Martin-Sotoca, J. J., Saa-Requejo, A., Orondo J. B., and Tarquis, A. M.: Singularity maps
668 applied to a vegetation index. Bio. Eng. 168, 42-53, 2018.
669 Motohka, T., Nasahara, K. N., Murakami, K., and Nagai, S.: Evaluation of sub-pixel cloud
670 noises on MODIS daily spectral indices based on in situ measurements, Remote Sens.,
671 3, 1644–1662, 2011.

Niemeyer, S.: New drought indices, First Int. Conf. on Drought Management: Scientific and Technological Innovations, Zaragoza, Spain. Joint Research Centre of the European Commission, Available online at http://www.iamz.ciheam.org/medroplan/zaragoza2008/Sequia2008/Session3/S.Niemeyer.pdf, 2008.

Ortega-Farias, S., Ortega-Salazar, S., Poblete, T., Kilic, A., Allen,R., Poblete-Echeverría, C., Ahumada-Orellana, L., Zuñiga,M., and Sepúlveda, D.: Estimation of Energy Balance Components over a Drip-Irrigated Olive Orchard Using Thermal and Multispectral Cameras Placed on a Helicopter-Based Unmanned Aerial Vehicle (UAV), Remote Sens., 8, 638, pp 18, 2016.

Park, S.: Cloud and cloud shadow effects on the MODIS vegetation index composites of the Korean Peninsula, Int. J. Remote Sens., 34, 1234–1247, 2013.

Rao, K. N.: Index based Crop Insurance, Agric. Agric. Sci. Proc., 1, 193–203, 2010.

Roumiguié, A., Sigel, G., Poilvé, H., Bouchard, B., Vrieling, A., and Jacquin, A.: Insuring forage through satellites: testing alternative indices against grassland production estimates for France, Int. J. Remote Sens., 38, 1912-1939, 2017.

Roumiguié, A., Jacquin, A., Sigel, G., Poilvé, H., Lepoivre, B., and Hagolle, O.: Development of an index-based insurance product: validation of a forage production index derived from medium spatial resolution fCover time series, GIScience Remote Sens., 52, 94-113, 2015.

Tackenberg, Oliver: A New Method for Non-destructive Measurement of Biomass, Growth Rates, Vertical Biomass Distribution and Dry Matter Content Based on Digital Image Analysis, Annals of Botany, 99(4), 777–783, 2007.

Turvey, C. G., and Mcaurin, M. K.: Applicability of the Normalized Difference Vegetation Index (NDVI) in Index-Based Crop Insurance Design, Am. Meorol. Soc., 4, 271-284, 2012.

UNEP Word Atlas of Desertification: Second Ed. United Nations Enviroment Programe, Nairobi, 1997.

USDA. U.S. Department of Agriculture, Federal Crop Insurance Corporation, Risk Management Agency: Rainfall Index Plan Annual Forage Crop Provisions. 16- RI-AF. http://www.rma.usda.gov/policies/ri-vi/2015/16riaf.pdf 2013 (Accessed March 1, 2018).

Wei, W., Wu, W., Li, Z., Yang, P., and Qingbo Zhou, Q.: Selecting the Optimal NDVI Time-Series Reconstruction Technique for Crop Phenology Detection, Intell. Autom. Soft. Co. 22, 237-247, 2016.